Journal of New Technology and Materials (JNTM)
J. New Technol. Mater.
Vol. 10, N°01 (2020)56-62

OEB Univ. Publish. Co.

Effect of cobalt chloride concentration on structural, optical and electrical properties of Co_3O_4 thin films deposited by pneumatic spray

Nabila Kouidri and Saâd Rahmane*

Laboratory of Physics of Thin Films and Applications, University of Biskra, BP 145 RP, 07000 Biskra, Algérie.

*Corresponding author : e-mail: rahmanesa@yahoo.fr, s.rahmane@univ-biskra.dz

Received date: Jan. 09, 2020; revised date: May 07, 2020; accepted date: May 10, 2020

Abstract

Cobalt oxide (Co_3O_4) thin films at different solution molarities (0.05, 0.1, 0.15, and 0.2mol/l) were successfully deposited on glass substrates by home-made pneumatic spray pyrolysis system (SPT) where the substrate temperature was maintained at 400 °C. Different techniques were used to study the properties of the deposited films. These are the X-Ray diffraction, UV-VIS spectroscopy, energy dispersive spectroscopy (EDS), scanning electron microscopy (SEM) and four probe points measurements. The obtained Co_3O_4 thin films are polycrystalline where the crystallites size increases from 19.53 to 26.11 nm when the molar concentration of Co precursor was increasing. SEM images revealed a uniform, homogeneous and well covered surface without any observable cracks. Peaks associated with Co and O elements are present in EDS analysis witch confirm the composition of the films. The transmittance spectra in the wavelength range of 300-2000 nm are used to study the optical properties. The optical band gap varied from 1.47 to 2.02 eV in the high energy region and from 1.41 to 1.45 eV in the low energy region. The electrical conductivity increased from $2.43*10^{-3}$ to $8.76*10^{-2}$ $(\Omega.cm)^{-1}$ with the increase of molarity.

Keywords: *thin film, Co_3O_4, pneumatic spray, molarity, properties.*

1. Introduction

Transition metal oxide (TMOs) are widely studied due to variable oxidation states of metal ions which facilitate redox transition making them good candidates for wide range of applications such as high charge storage in supercapacitor and water decomposition [1]. Because its low cost, environmentally friendly nature, availability, different oxidation states, redox reversibility, mixed capacitive behavior, large potentials window, good electrical conductivity, and different morphologies [2], cobalt oxide is one of the promising material as transpatrent conductor oxide (TCO). In general, cobalt oxide exists in three different crystalline forms CoO, Co_2O_3 and Co_3O_4[3]. Cobalt monoxide is the final product formed when cobalt compounds or oxides are calcinated to a sufficiently high temperature (1173 °K). The pure CoO is difficult to obtain since it readily takes up oxygen even at room temperature to reform to a higher oxide. Cobaltic oxide (Co_2O_3) could be formed when cobalt compounds are heated at a low temperature in the presence of an excess of air. Some authors have reported that Co_2O_3 exists only in the hydrated form [4]. At a temperature higher than 538 °K, Co_2O_3 can be completely converted into Co_3O_4. In sufficient quantity of oxygen, Co_2O_3 transforms to a higher oxide Co_3O_4 with no change in the lattice structure [4] which is reported for the electrochemical applications because of its chemical stability [5]. With normal spinel structure of AB_2O_4 type where Co^{2+} ions occupy the tetrahedral 8a sites and Co^{3+} occupy the octahedral 16d sites [6], it acts like a p-type semiconductor. Co_3O_4has been extensively studied in the fields of solar selective absorbers [7,8], anodic electro-chromic materials in smart window devices, negative electrodes in lithium-ion batteries [9], rechargeable batteries[10], sensing[11], protective layers or pigment for glasses, ceramics [12], effective catalyst in environmental purification and chemical engineering [13]. Thin films of Co_3O_4 are prepared on a variety of substrates by different methods such as RF sputtering [14], pulsed laser deposition [15], sol gel process[3], spray pyrolysis [2] and chemical vapor deposition [16].

Because of its simplicity and low cost, spray pyrolysis deposition technique is used in this work to prepare Co_3O_4 films. Naturally, the properties of the deposited cobalt oxide thin films are dependent on solvents, the nature of used precursors, and the processing conditions.

The aim of this work is to investigate the effect of cobalt amount concentration in precursor solution on the structural, optical and electrical properties of Co_3O_4 thin films deposited by spray pneumatic. X-ray diffraction analysis (XRD), UV–VIS spectroscopy,

energy dispersive spectroscopy (EDS), scanning electron microscopy (SEM) and four probe point conductivity method are used to study the effect of cobalt starting solution concentration on Co_3O_4thin films properties.

2. Experimental details

The Cobalt oxide films were prepared using a home-made spray pyrolysis experimental setup [17]. The precursors; Cobalt chloride ($CoCl_2$) dissolved in distilled water in our case, were sprayed by atomization processes then condensed onto the heated substrates. The solution is prepared in 0.05, 0.1, 0.15 and 0.2 mol/l as molar concentrations. Glass substrates (TLC Silica gel 60 F_{254}) were used to deposit the films. The substrate working temperature was fixed at 400°C.

The possible chemical reaction for the formation of Co_3O_4 films is shown in the following equation [18]:

$$3CoCl_2 + 2H_2O + O_2 \rightarrow Co_3O_4 \downarrow +3Cl_2 \uparrow +2H_2 \uparrow \quad (1)$$

When the cobalt chloride ($CoCl_2$) is dissolved in distilled water, it forms cobalt hydroxide and it is fully decomposed into cobalt oxide at substrate temperature above 400°C where the ambient air is playing the main role in the formation of Co_3O_4phase [19].

Preparation procedure of solution and substrates, the structural and crystalline properties, the morphology and the chemical composition, the optical transmission and the electrical conductivity of the films measurements are detailed in [20].

3. Results and discussions

The deposited films are physically stable and have a good adherence onto the glass substrates.

3.1. Film thickness

The thickness of the deposited films can be estimated using the gravimetry method which consists in measuring the change in weight of the substrate due to film deposition using an electronic high-precision balance. Knowing the area of film and the density of Co_3O_4 (6.2 g/cm3) [13], the film thickness d is determined as follows [21]:

$$d = {}^{m}/_{(A * \rho)} \quad (2)$$

Where A, m and ρ are the surface area, the mass and the density of Co_3O_4respectively.

From figure (1) we can notice that the growth velocity have a similar trend of variation with the rise in molar concentration. The continuous increase in growth velocity with precursor concentration indicates that the growth velocity may be governed by the Co-containing species. It is difficult to control the incorporation of O^{2-} into the film during the growth process using the spray pyrolysis technique. The atmospheric conditions where the film growth takes place can't controlled accurately and hence the stoichiometry is only controlled by the Co species.

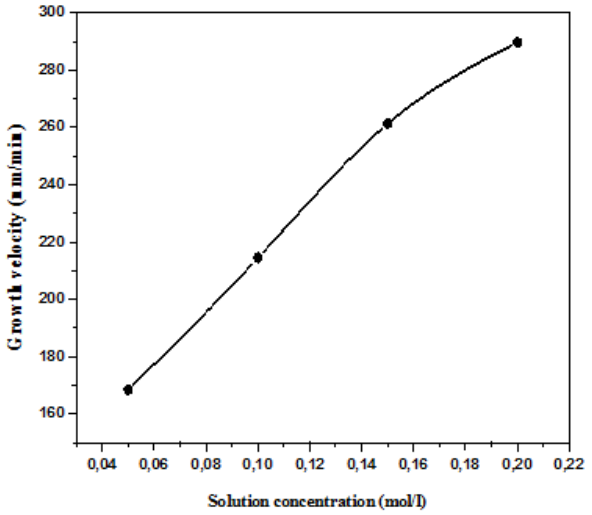

Figure 1. Plot of growth velocity versus molar concentration.

3.2. Structural Properties

The shape and type of the lattice structure of Co_3O_4 thin films were carried out by X-ray diffraction technique and the patterns of the films with a various molar concentration (0.05, 0.1, 0.15, and 0.2 mol/l) are shown in figure 2. It is clear that all films show many diffraction peaks at 2θ = 19.46°, 31.68°, 37.27°, 38.77°, and 59.52° correspond to (111), (220), (311), (222) and (511) plane respectively. That indicates that the Co_3O_4 films are polycrystalline. Their cubic spinel structure is confirmed when compared to the JCPDS card N°: 00-042-1467 which belongs to the space group Fd3m. The film deposited with the higher concentration of 0.2 mol/l solution shows an additional peak at 44.97° denoting reflection from (400) plane. The other possible crystalline phases such as Co_2O_3, CoO etc. are not detected; thus proving that the only formed phase is the spinel cobalt oxide and the formed Co_3O_4 phase is found to be stable because. Noting the peak intensity, the crystallinity of the sample depends on the thickness of the films which in turn are affected by the solution concentration. The results show that the film deposited at 0.2 mol/l is thicker than the films deposited at lower molar concentration, more lattice planes are available for initiating diffraction of incident X-rays. As the thickness of the films increases, the X-ray peak intensity also increased. From figure 2, the peaks intensity gradually increases with spraying solution concentration; this increase is possibly caused by the increase of the level of crystallization due to the rise of the amount of impinging Co species primarily present in the solution source. All the deposited films have the (111) orientation as the preferred one. This behavior can be attributed to the density of atoms in (111) plane where the surface energy of this plane is the lowest [20]. The atoms of films that which deposited later will arrange

themselves in the direction of the lowest internal energy in order to get rid of its excess energy and to reach to the stable state.

The sequence of atoms arranging themselves in that direction (111) [23]. The intensity of the peak (111) is increases with increasing the solution concentration; it becomes intense at the concentration of 0.2 mol/l due to the maximum thickness of films (see table 1) at higher cobalt chloride concentrations as obtained by Rahmane [24], Kamalianfar [25] and Bhavana [26] for the ZnO films prepared by magnetron sputtering, pulsed laser deposition and electrostatic spray respectively, thus indicating that the films crystallinity has been improved.

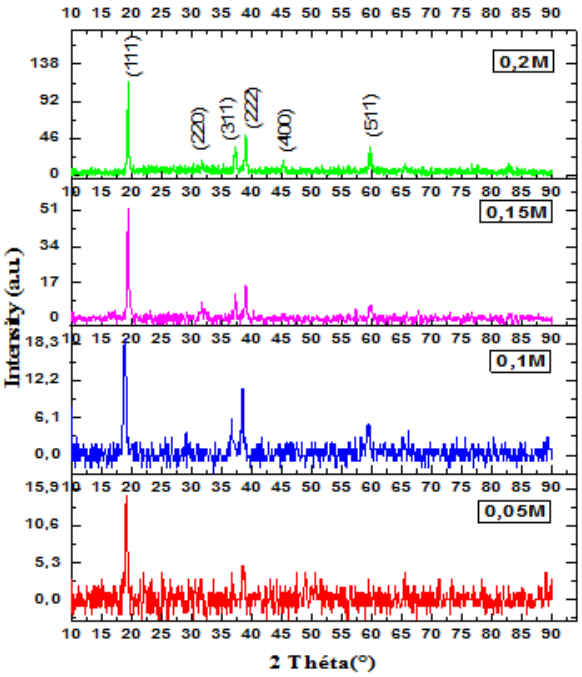

Figure 2. X-ray diffraction patterns of Co_3O_4 thin films with different molar concentration.

Moreover, we notice from table (1), that there is a variation in lattice parameter 'a' and small difference in the position of the (111) diffraction peak (variation in the value of the angle diffraction 2θ) that is probably caused by the manifestation of the stress during the films growth.

Table 1: Values of lattice parameters 'a', interplanar distance'd', thickness 't' and intensity '$I_{(111)}$' of Co_3O_4thin films.

M (mol/l)	t (nm)	2θ (°)	d_{hkl} (Å)	a (Å)	$N*10^{14}$ (cm^{-2})	$I_{(111)}$ (a.u)
0.05	505.29	19.178	4.63003	8.01945	6.57	13.896
0.1	643.47	18.939	4.68632	8.11695	8.62	19.046
0.15	784.05	19.485	4.55615	7.89148	4.71	49.733
0.2	869.22	19.460	4.56154	7.90082	3.76	91.661

The size of the formed Co_3O_4 crystallites is estimated by applying Scherer method to the (111) peak where FWHM is directly measured from the XRD data. As known, dislocations and strain modify the surface properties of the films, to get the values of the crystallite size (D), the dislocation density (δ) and strain (ε) the following formulas are applied [20]:

$$D = \frac{0.9\lambda}{\beta cos\theta} \quad (3)$$

$$\delta = \frac{1}{D^2} \quad (4)$$

$$\varepsilon = \frac{\beta cos\theta}{4} \quad (5)$$

The variations of the crystallite size (D), the dislocation density (δ) and strain (ε) with respect to the solution concentration are illustrated in Figure 3.

The crystallite size of the (111) surface varies from 19.53 to 26.11 nm. The figure 3 show clearly that the crystallite size increases as the molar concentration increases. A possible interpretation of this fact is that; in one hand and, the number of cobalt ions reaching the substrate where cobalt atoms condensate at higher rate and faster nucleation of the crystallites results into the formation of bigger grains which confirms also the increase of growth velocity in the other hand (see figure 1).

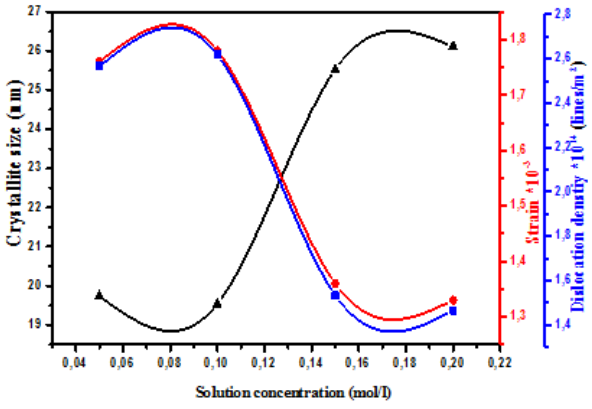

Figure 3. The variation of crystallite size (D), dislocation density (δ) and strain (ε) as a function of molar concentration.

Furthermore, the dislocation density and strain are decreasing with the increase of molar concentration, and inversely with the crystallite size. The decrease of both and strain dislocation density shows that the lattice imperfections become less important along grain boundaries. The crystallites sizes, strain and dislocation density are in good agreement with those reported by Manickam [19] and Ravi Dhas [27].

The density of crystallites (N) is estimated based on the following formula [28]:

$$N = \frac{t}{D^3} \quad (6)$$

The number of crystallites per unit of volume into Co_3O_4 thin films is reported in Table.1. The values of N reveal a clear decrease as the solution concentration increases which is probably due to the increase of nucleation rate and growth velocity onto the surface of the substrate. A similar interpretation is given by Prabu [28].

One of the basic structural parameters of polycrystalline materials is the texture coefficient (TC) which represents the texture of a particular plane. If TC is greater than unity, then there are numerous of grains in that particular direction. The texture coefficients $TC_{(hkl)}$ for all samples is calculated from the X-ray diffraction data using the formula [22]:

$$TC = \frac{I_{hkl}}{\frac{1}{N}\sum I_{hkl}} \quad (7)$$

Where I(hkl) denotes the X-ray reflection measured intensity in the (hkl) direction, and N is the number of reflections present in the XRD patterns.

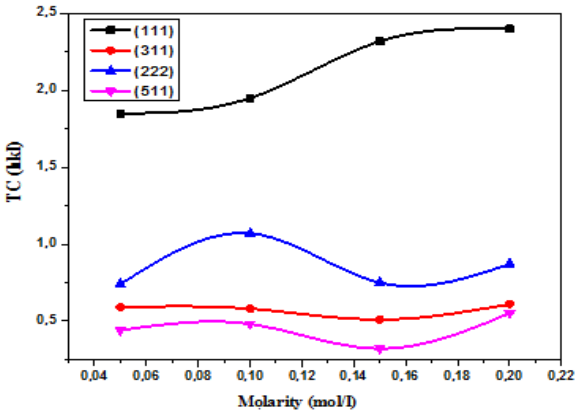

Figure 4. Texture coefficient as a function of molarity.

The dominance of Co_3O_4 phase (111) plane for all molarities is clear as indicates figure 4. All values of texture coefficient are greater than 1 indicating the abundance of grains in that direction. An opposite trend for the texture coefficients of (311), (222), and (511) is remarked where a possible transfer of grains as a function of molarity between the four orientations. The texture coefficient TC(111) is found to increase from 1.85 to 2.4. The increase in the molar concentration leads necessarily to an increase of the arriving species (cobalt and oxygen) to the surface during the film growth resulting in an abundance of the grains. The EDS data agrees well as shown in figure 6 where an increase in cobalt chloride concentration is observed and it is very likely giving rise to (111) preferential orientated thin films.

3.3. Morphological and elemental analysis

The surface morphology of the Co_3O_4 thin films deposited at different molar concentration is investigated by scanning electron microscopy (SEM). As Figure 5 shows, the SEM surface images of the Co_3O_4 indicate the polycrystalline and porous nature. The micrographs clearly illustrate the formation of sub-micrometer crystallites distributed in a uniform manner over the surface. Although the films are well recovered and no cracks could be detected, some holes are present. The amount of solute increases in the solute as the concentration increases and therefore the electrostatic interaction between the solute particles becomes larger. As a result an increasing in the probability of gathering more solute to form bigger grains this in turn leads to a rougher surface of the grown films. In the other side, it seems that agglomerations of small crystallites are present in certain regions on the film surface, especially at the greater molar concentrations (See (c) and (d) micrographs). The observed increase in surface area due to the present surface morphology of our films is suitable for super-capacitor and gas sensing applications as reported by [29].

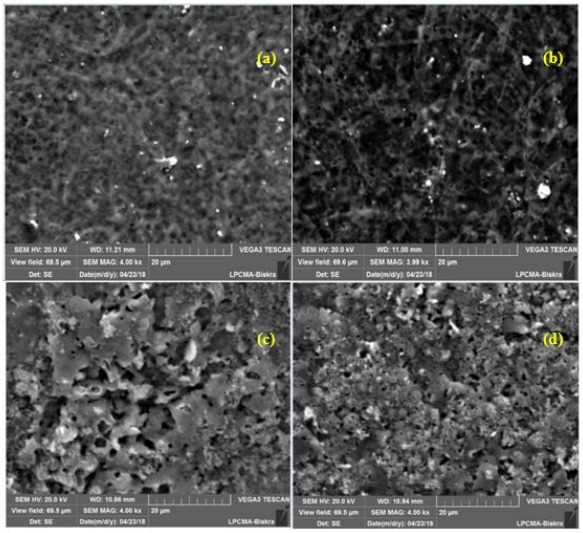

Figure 5. SEM surface images of the Co_3O_4 thin films deposited at various molar concentration: (a) 0.05, (b) 0.1, (c) 0.15 and (d) 0.2mol/l.

The EDS compositional analysis of Co_3O_4 films is shown in figure 6. This spectrum confirms the presence of Co and O elements in the Co_3O_4 films prepared by different solution concentrations. The presence of silicon and carbon peaks may arise from the glass substrate contamination respectively. The cobalt content increases as the molar concentration increases which is due to rise of its atomic percentage whereas the increase in oxygen content could be attributed to the chemisorbed oxygen from the atmospheric air [27].

3.4. Optical properties

Transmittance spectrums of the deposited Co_3O_4 thin films were recorded at room temperature in the wavelength range 300-2000 nm. From figure 7, it is seen that transmittance decreases with the increase of solution concentration. The reduction of transmittance at higher molar concentration is due to the increase in the thickness of the films, as the density of the atoms leads to more optical scattering phenomenon in Co_3O_4 [27]. The transmittance increases up to wavelength 624 nm and then decreases up to 737 nm and again increases from 1100 nm, depicting two regions of optical

transitions. Absorption bands are assigned to the charge transfer of $O^{-2} \rightarrow Co^{+3}$ at lower energy region and $O^{-2} \rightarrow Co^{+2}$ at higher energy region [30]. Co_3O_4 is known to show strong optical absorption in the visible region which is easily evident from its dark black color.

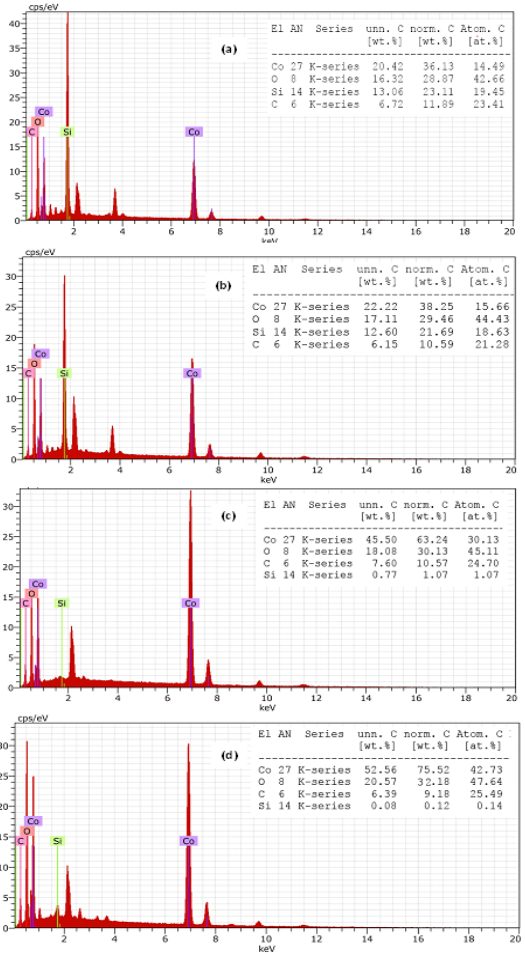

Figure 6: EDS spectrums of Co_3O_4 films deposited under different molarities: (a) 0.05, (b) 0.1, (c) 0.15 and (d) 0.2 mol/l.

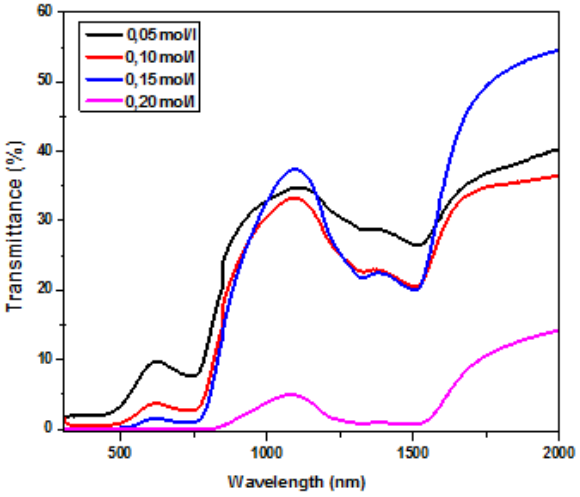

Figure 7. Optical transmittance spectra of Co_3O_4 thin films as a function of the wavelength for different molarities.

The optical absorption coefficient **α** is determined from the transmission data as reported in previous works [22, 26]. As can be seen in table 2, the absorption coefficient increases with the increase of solution concentration. The values are greater than 10^4 cm^{-1}, suggesting a high probability of the occurrence of direct transitions [31, 32] since they are responsible for good electrical conduction [33].

Is known that good absorbing light semiconductors in this region of solar spectrum are desired for a practical conversion from incident photons which have enough energy for the occurrence of electron transitions [34]. The energy gap is calculated using following classical relation for optical absorption in semiconductors given in [35]:

$$\alpha h\upsilon = A(h\upsilon - E_g)^n \qquad (8)$$

Where, A is a constant, Eg the semiconductor band gap and 'n' is a number equal to 0.5 for the direct gap and 2 for indirect gap compounds. Two linear regions appear indicating the existence of two different band gap energy values, which may be attributed to the spin-orbit splitting of the valence band. The extrapolation of two straight lines to $(\alpha h\nu)^2 = 0$ give values of the direct band gaps of Co_3O_4 thin films. Obtained Eg values are given in table 2. As seen from this table, the low values of the energy band gap varies between 1.41 and 1.45 eV while the high values which are obtained from the extrapolation of the first linear region found to be varying between 1.47 and 2.06 eV. Analogous results are reported by Manickam (Eg_1 =1.5609–1.3636 eV , Eg_2 =2.885–2.3435 eV) [19], Pal (Eg_1 =1.57 eV , Eg_2 =2.28 eV) [36], and Lakehal (Eg_1 = 1.50 *eV*, Eg_2 = 2.20 *eV*) [37] which suggest the possibility of the degeneracy of the valence band.

Urbach tail (Eu) characterizing the width of the localized states available in the optical band gap of the films affects the optical band gap structure and optical transitions. It is directly related to a similar exponential tail for the density of states of either one of the two band edges [34]. The values of (Eu) were obtained from the inverse of the slope of (ln**α**) versus (h**υ**) according to the following relation [35]:

$$\alpha = \alpha_0 . \exp(\frac{h\upsilon}{E_u}) \qquad (9)$$

We notice that the Eg_1 and Eg_2 values increase when the molarity increases up to 0.15mol/l and then Eg_2 decrease at 0.2 mol/l. Allag [17] returns the increase of band gap to the Burstein–Moss effect when the solution concentration increase (thickness of film increase), however Dutta [38] considers that the decrease in the band gap can be related with the decreasing trend in the strain for which the interatomic spacing of semiconductors affects the energy gap. In addition, Manickam [19] and Alami [39] explained the decrease in band gap by the increase in carrier concentration; however Agbogu [3] clarifies this decrease by the increase of crystallite size deposited at high precursor

concentrations. Moreover, the increase of Urbach energy for high concentration (0.2 mol/l) contributes to the decrease of energy band gap; since Urbach energy values change inversely with optical band gap as shown in table 2.

Therefore, it is clear that the elaborated sample using 0.15 - 0.2 mol/l, has low band gap energy and strong absorption at lower wavelengths. These films have a potential for the application as an absorber layer in solar cell fabrication [40].

Table 2: The electrical and optical parameters values of the deposited Co_3O_4 thin films.

M (mol/l)	$R_{sh}*10^5$ (Ω)	σ $(\Omega.cm)^{-1}$	Eg_1 (eV)	Eg_2 (eV)	Eu_1 (eV)	Eu_2 (eV)	$\alpha*10^4$ (cm^{-1})
0.05	17.9	0.00243	1.41	1.92	0.12	0.28	6.146
0.1	13.2	0.00258	1.44	1.94	0.11	0.26	6.654
0.15	1.46	0.01925	1.45	2.02	0.08	0.17	11.93
0.2	0.29	0.0876	/	1.47	/	0.29	15.67

3.5. Electrical properties

For all Co_3O_4 thin films, the four-point probe is used for the measurement of sheet resistance (R_{sh}). A fairly accurate estimation of R_{sh} using the following relation [22]:

$$R_{sh} = 4.532\ (V/I) \quad (10)$$

The conductivity (σ) values of films are calculated from the following formula:

$$\sigma = 1/(R_{sh}.t) \quad (11)$$

Where t is the thickness of the film.

The values of electrical conductivity (σ) and sheet resistance (R_{sh}) of Co_3O_4thin films are listed in Table 2. Figure 8, shows the dependence of electrical conductivity (σ) and absorption coefficient on solution concentration.

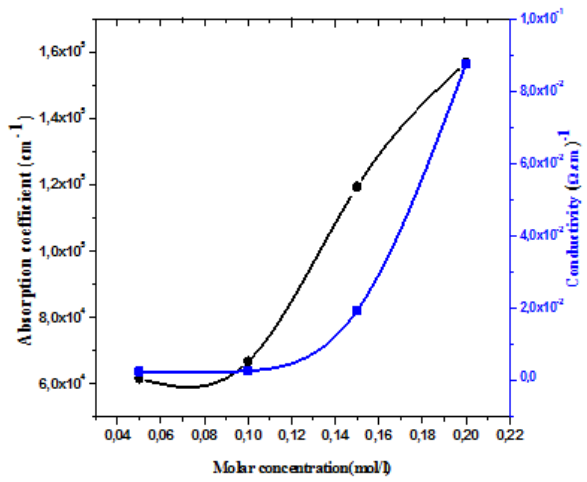

Figure 8. Electrical conductivity and absorption coefficient variations of Co_3O_4 thin films as a function of precursor molarity.

As it can be seen, the electrical conductivity increases continuously with increase in the solution concentration and its values varied from $2.43*10^{-3}$ to $8.76\ *10^{-2}\ (\Omega.cm)^{-1}$. This increase is mainly attributed to the increasing of carrier concentration (holes). The observed low-resistivity with the increasing the absorption coefficient is attributed to the increase of the holes concentration in the valence band due to the electronic transitions to the conduction band and the holes induced by the non-stoichiometry of oxygen lattice in p-type Co_3O_4 grains [20].

4. Conclusion

The effect of molar concentration on structural, morphological, optical and electrical properties of Co_3O_4 thin films deposited on glass substrates by home-made pneumatic spray pyrolysis system is studied. X-ray diffraction reveals a polycrystalline nature for all films with a preferred grain orientation along to (111) plane when the solution concentration changes from 0.05 to 0.2 mol/l. Crystallites sizes of the films have been found to be increasing from 19.53 to 26.11 nm, leading to the enhancement in the crystallinity. The SEM micrographs clearly illustrate the formation of sub-micrometer crystallites distributed more or less uniformly over the surface. Although films are well recovered and no cracks could be detected, some holes indicating porosity are present. The transmittance of the prepared thin films decreases as the solution concentration increases. The results of the optical analysis showed that there are two linear regions indicating the existence of two different band gap energy values suggesting a spin-orbit splitting of the valence band. The values of the energy band gap varied between 1.41 and1.45 eV in low energy region while in high energy region the energy band gap values varied between1.47 and 2.02 eV.

The electrical conductivity of the deposited thin films increases from $2.43*10^{-3}$ to $8.76\ *10^{-2}\ (\Omega.cm)^{-1}$ with solution concentration, this increase is mainly attributed to the increase of carrier concentration (holes). Finally, the present work clearly indicated that the molarity is an important parameter and affects significantly the physical properties of Co_3O_4 films. These properties demonstrate that the Co_3O_4 films which are deposited especially using 0.15 – 0.20 mol/l concentration are a promising material as an absorber layer in photovoltaic and gas sensing applications.

References

[1] S. K. Meher, G. R. Rao, J. of Physical Chemistry, 115(2011) 15646-15654.

[2] R.C. Ambare, S. R. Bharadwaj, B. J. Lokhande, I.J.S.N., 5(4) (2014) 663-668.

[3] A.N.C. Agbogu, A.B.C Ekwealor, F.I. Ezema, Digest Journal of Nanomaterials and Biostructures, 9(3) (2014) 1289 – 1296.

[4] V.R. Shinde, S.B. Mahadik, T.P. Gujar, C.D. Lokhande, Applied Surface Science, 252(2006) 7487–7492.

[5] A. Louardi, T. Chtouki, A. Rmili, B. Elidrissi, H. Erguig, International Journal of Applied Engineering Research, 11(2) (2016)1432-1435.
[6] Lu Pan, Zude Zhang, J Mater Sci: Mater Electron, 21(2010)1262–1269
[7] Mehdi Rahimi-Nasrabadi, Hamid Reza Naderi, Meisam Sadeghpour Karimi, Farhad Ahmadi, Seied Mahdi Pourmortazavi, J Mater Sci: Mater Electron, 28(2017) 1877.
[8] Saad Oboudi, International Journal of Innovative Research in Science, Engineering and Technology, 3(1) (2014) 8573-8581.
[9] A. B. C. Ekwealor, S. U. Offiah, S. C. Ezugwu, and F. I. Ezema, Indian Journal of Materials Science, Volume 2014(2014), Article ID 367950, 5 pages.
[10] Sami S. Chiad, Saad F. Oboudi, Jubair. A. Najim, Nadir F. Habubi, *J. of uni. of Anbar for pure sc.* **7(2)** (2013).
[11] Romana Drasovean, Simona Condurache-Bota, Nicolae Tigau, Journal of Science and Arts, 2(13) (2010) 379-384.
[12] P.N. Shelke, Y.B. Khollam, K.R. Patil, S.D. Gunjal, S.R. Jadkar, M.G. Takwale, K.C. Mohite , J. Nano- Electron. Phys. 3(1) (2011) 486-498.
[13] Vikas Patil, Pradeep Joshi, Manik Chougule, Shashwati Sen, Soft Nanoscience Letters, 2(2012) 1-7.
[14] C.L. Liao, Y.H. Lee, S.T. Chang, K.Z. Fuang, J. Power Sources, 158(2006) 1379.
[15] S Z Abbas, A A Aboud, M Irfan and S Alam, Materials Science and Engineering 60(2014) 012058.
[16] D. Barreca, C. Massignan, S. Daolio, M. Fabrizio, C. Piccirillo, L. Armelao, E. Tondello, Chem. Mater. 13(2001) 588–593.
[17] Allag Abdelkrim, Saâd Rahmane, Ouahab Abdelouahab, Nadjate Abdelmalek, Gasmi Brahim, Optik 127(2016) 2653–2658.
[18] V.R. Shinde, S.B. Mahadik, T.P. Gujar, C.D. Lokhande, Applied Surface Science 252(2006) 7487–7492.
[19] M. Manickam, V. Ponnuswamy, C. Sankar, R. Suresh, Optik, 127(2016) 5278–5284.
[20] Kouidri Nabila, Saâd Rahmane and Allag Abdelkrim, J Mater Sci: Mater Electron (2018). https://doi.org/10.1007/s10854-018-0384-3
[21] Allag Abdelkrim, Saâd Rahmane, Kouidri Nabila, Attouche Hafida, Ouahab Abdelouahab, J Mater Sci: Mater Electron 28(2017)4772–4779.
[22] Allag Abdelkrim, Saâd Rahmane, Ouahab Abdelouahab, Attouche Hafida, and Kouidri Nabila, Chin. Phys. B, 25(4) (2016) 046801.
[23] Sameer A. Maki, Bushra K. Hasson, Tahir H. Mahmoud, Journal of Multidisciplinary Engineering Science Studies (JMESS), 3(4) (2017)1644-1650.
[24] Saâd Rahmane, Mohamed Salah Aida, Mohamed Abdou Djouadi, Nicolas Barreau, Superlattices and Microstructures, 79(2015) 148–155.
[25] A. Kamalianfar, S. A. Halim, Kasra.Behzad, Mahmoud Goodarz Naseri, M. Navasery, Fasih Ud Din, J. A. M. Zahedi, K.P.Lim, S.K.Chen, H.A.A.Sidek, Journal Of Optoelectronics And Advanced Materials, 15(3 – 4) (2013) 239 – 243.
[26] Bhavana N. Joshi, Hyun Yoon, Ho Young Kim, Joon Ho Oh, Tae Yeon Seong, Scott C. James, and Sam S. Yoon, Journal of The Electrochemical Society, 159 (8) (2012) H716-H721.
[27] C. Ravi Dhas, R. Venkatesh, R. Sivakumar, A. Moses Ezhil Raj, C. Sanjeeviraja, Optical Materials, 72(2017) 717-729.
[28] R. David Prabu, S. Valanarasu, V. Ganesh, Mohd Shkir, S. AlFaify, A. Kathalingam, Surf. Interface Anal. 50(2018) 346–353.
[29] Sabah Habeeb Sabeh, Eng. &Tech. Journal, 34(B4) (2016) 553-559.
[30] O. Gencyılmaz,T. Taskopru, F. Atay, I. Akyuz, Appl. Phys. A, 121(1) (2015) 245–254.
[31] Nabeel A. Bakr, Sabah A. Salman and Ahmed M.Shano, International Journal of Current Research, 6(11) (2014) 9644-9652.
[32] H.H. Daroysh, AL-Muthanna J. Pure Sci. (MJPS) 3(2) (2016) 285-294.
[33] A.Elsakhi S. M. Hamed, Mohamed A. Siddig, Abdelrahman A. Elbadawi, Asmma I. Mohamed, M.Elhadi, International Journal of Scientific Research and Innovative Technology, 2(5) (2015) 112-116.
[34] Nabeel A. Bakr, Sabah A. Salman, Ahmed M. Shano, International Letters of Chemistry, Physics and Astronomy, 41(2015) 15-30.
[35] Saad Rahmane, Mohamed Abdou Djouadi, Mohamed Salah Aida, Nicolas Barreau, Thin Solid Films, 562(2014) 70–74.
[36] Jagriti Pal, Pratima Chauhan, MATERIALS CHARACTERIZATION, 61(2010) 575–579.
[37] Abdelhak Lakehal, Benrabah Bedhiaf, Amar Bouaza, Hadj Benhebal, Abdelkader Ammaric, Cherifa Dalache , Materials Research, 21(3) (2018) e20170545.
[38] M. Dutta, S. Mridha, D. Basak, Applied Surface Science, 254(2008) 2743–2747.
[39] Z.Yamlahi Alami, M. Salem, M. Gaidi, J.Elkhamkhami, Advanced Energy: An International Journal (AEIJ), 2(4) (2015) 11-24.
[40] Mehdi Dhaouadi, Mohamed Jlassi, Imen Sta, Islem Ben Miled, George Mousdis, Michael Kompitsas, Wissem Dimassi, American Journal of Physics and Applications, 6(2) (2018) 43-50.